Electronic Supporting Information

Highly efficient Pb(II) and Cu(II) removal using hollow Fe_3O_4@PDA nanoparticles with excellent application capability and reusability

Ning Wang [a,b], Dongxu Yang [a,b], Xiangxue Wang [b,c], Shujun Yu [b], Hongqing Wang *[a], Tao Wen [b], Gang Song [c], Zhimin Yu [d] and Xiangke Wang *[b,d]

* Corresponding authors

[a] School of Chemistry and Chemical Engineering, University of South China, 28 Changsheng West Road, Hengyang, Hunan 421001, PR China

E-mail: Hqwang2001cn@126.com

[b] College of Environmental Science and Engineering, North China Electric Power University, Beijing 102206, PR China

E-mail: xkwang@ncepu.edu.cn

[c] Guangdong Provincial Key Laboratory of Radionuclides Pollution Control and Resources, Guangzhou University, Guangzhou, 510006, China

[d] Department of Biology and Environmental Engineering, Hefei University, Hefei 230000, PR China

2. Experimental

2.1. Chemicals

All chemicals (lead nitrate ($Pb(NO_3)_2$), copper nitrate ($Cu(NO_3)_2$), ferric chloride hexahydrate ($FeCl_3 \cdot 6H_2O$), dopamine (DA), polyacrylamide (PAM), sodium citrate ($Na_3C_6H_5O_7 \cdot 2H_2O$), urea ($CH_4N_2O$), sodium nitrate ($NaNO_3$), ethanol ($C_2H_5OH$), concentrated nitric acid (HNO_3), sodium hydroxide (NaOH)) were obtained form

sinopharm chemical reagent Co, Ltd in analytical grade, and used without further purification.

2.4. Characterization

The structures and surface morphologies of the as-prepared materials were characterized by field emission scanning electron microscopy (FE-SEM, Hitachi s-4800) and transmission electron microscopy (TEM, jeol 200f). The X-ray diffraction (XRD) measurements were carried out on D/max2500, utilizing a Cu K_{α} source (λ= 1.541 Å) at a scanning speed of 6º/min at the measuring region from 5º to 70º. Information regarding functional groups was measured on Fourier transformed infrared spectroscopy (FT-IR, IR Tracer-100). Thermogravimetric analyses (TGA) were performed by using the SETSYS Evolution thermo analyzer under N_2 atmosphere with a heating rate of 10 °C min^{-1} from ambient temperature to 800 °C. Magnetic properties of adsorbents were analyzed by vibrating sample magnetometer (VSM, EV7, ADE) with an applied magnetic field between -10000 and 10000 O_e at ambient temperature. Based on the binding energy of samples, X-ray photoelectron spectroscopy (XPS, hermo Escalab 250) was conducted via adopting an Al X-ray source operated at 10 kV. The Zeta potential values of Fe_3O_4@PDA were achieved via a dynamic light scattering on ZETASIZER 3000 HAS system.

Figures captions

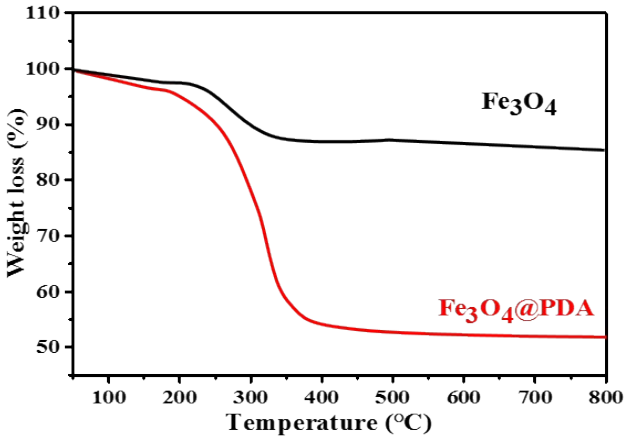

Fig. S1. TGA curves of Fe_3O_4 and Fe_3O_4/PDA nanoparticles.

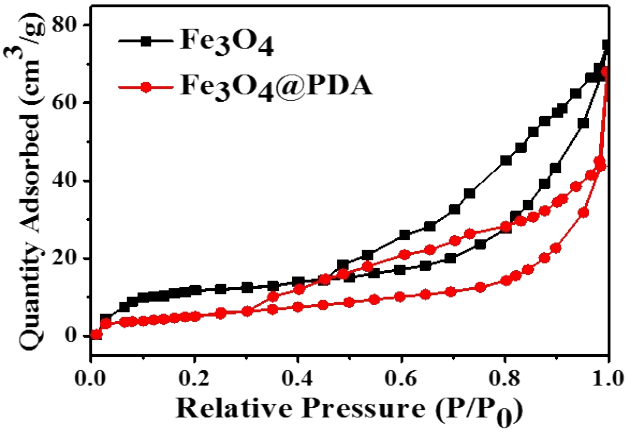

Fig. S2. Nitrogen adsorption-desorption isotherm plot of hollow Fe_3O_4 microspheres and Fe_3O_4@PDA nanoparticles.

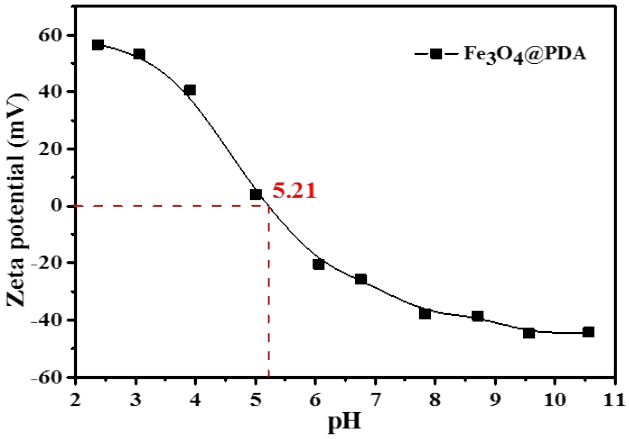

Fig. S3. Zeta potential values as a function of pH. *T*= 298 K, m/V= 0.2 g·L^{-1}.

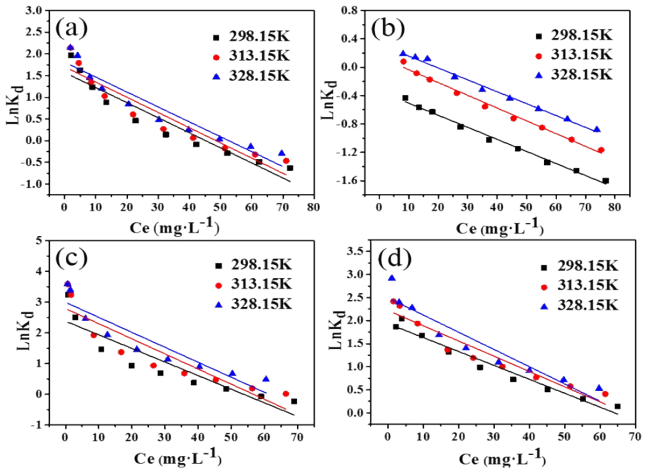

Fig. S4. The linear plots of lnK_d versus C_e curves of Pb(II) (a) and Cu(II) (b) adsorption on Fe_3O_4, and Pb(II) (c) and Cu(II) (d) adsorption on Fe_3O_4@PDA.

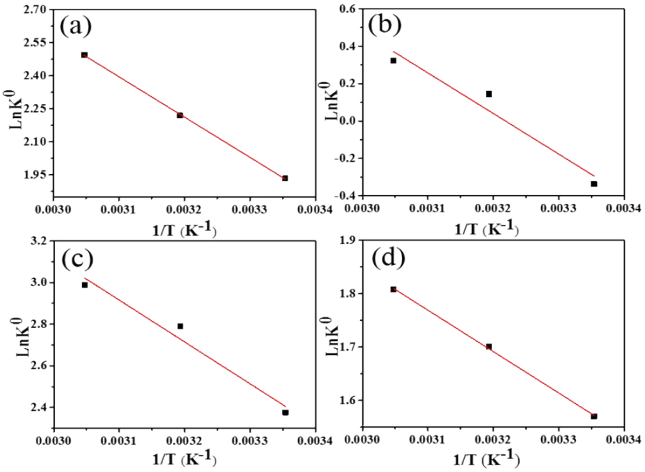

Fig. S5. The linear plots of lnK^0 versus $1/T$ of Pb(II) (a) and Cu(II) (b) adsorption on Fe_3O_4, and Pb(II) (c) and Cu(II) (d) adsorption on Fe_3O_4@PDA.

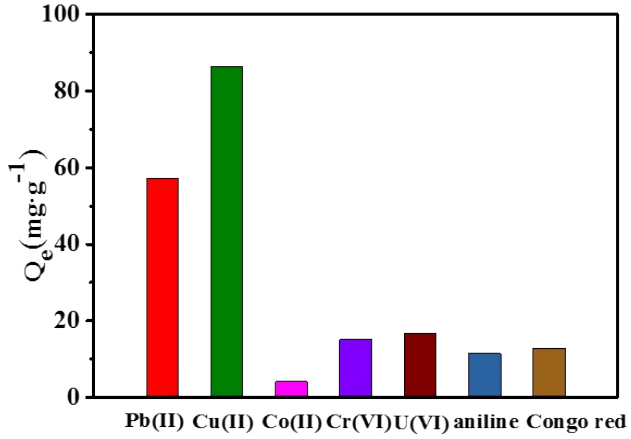

Fig. S6. The adsorption capacities of Fe_3O_4@PDA for seven adsorbates, m/V = 0.2 $g \cdot L^{-1}$, I = 0.01 M $NaNO_3$, $C_{0\ [initial]}$=10 $mg \cdot L^{-1}$, T = 298 K.

Table. S1. Adsorption thermodynamic parameters of Pb(II) and Cu(II) on Fe_3O_4 and Fe_3O_4@PDA at different temperatures

Adsorbents	Metal ions	*T*(K)	ΔG^0(kJ·mol^{-1})	ΔS^0(J·K^{-1}·mol^{-1})	ΔH^0 (kJ·mol^{-1})
Fe_3O_4	Pb(II)	298	-10.33	36.67	6.64
		313	-10.85		
		328	-11.37		
	Cu(II)	298	-17.29	58.08	18.04
		313	-18.16		
		328	-19.04		
Fe_3O_4@PDA	Pb(II)	298	-22.65	76.03	16.71
		313	-23.79		
		328	-24.93		
	Cu(II)	298	-19.97	67.04	15.19
		313	-20.97		
		328	-21.98		